

Satellite Clock Bias Prediction Based on Metabolizing GM(1,1) and BP Neural Network

Jianlong Cheng, Ye Yu*, Guodong Jin, Jianwei Zhao, Xiaoyu Gao, Minli Yao

Rocket Force University of Engineering, Xi'an, 710025, Shaanxi, China

*Corresponding author: yuye115@mails.ucas.edu.cn

Abstract: This study proposes a hybrid satellite clock bias prediction method combining the metabolizing GM (1,1) model and a BP neural network: GM (1,1) provides initial short-term forecasts; residuals between predictions and true values are modelled by the BP network; final predictions are obtained by adding BP-predicted residuals to GM (1,1) outputs. Validated on eight GPS satellite clocks using high-precision products from Wuhan University's GNSS Analysis Centre, the method achieves superior accuracy and stability over standalone models. The hybrid model attains average error of 1.14 ns and stability of 2.04 ns—improving accuracy by 19.72% relative to the linear polynomial model and by 15.56% relative to the grey model, and improving stability by 21.54% relative to the linear polynomial model and by 17.07% relative to the grey model.

Keywords: Linear polynomial model; Grey model; Metabolism; BP neural network; Satellite clock bias; Forecast

1. Introduction

The Global Navigation Satellite System (GNSS) is a system centered on time measurement. A 1 ns time measurement error can lead to a 30 cm ranging error. The onboard atomic clock, as an important payload of navigation satellites, is responsible for establishing and maintaining the time reference for onboard units and is the “heart” of GNSS satellites. Its performance directly affects the accuracy and availability of positioning, navigation and timing services. Although atomic clocks can demonstrate high precision levels with their excellent performance, maintaining high-precision clock error data faces enormous challenges when facing the extreme harsh environment of space [1-2].

A wealth of international and domestic research has established solid theoretical frameworks and diverse models for satellite atomic clock bias prediction, including LPM, QPM, GM (1,1), Kalman filtering, and Spectrum Analysis methods [3-8]. Polynomial models offer low complexity and high short-term accuracy but degrade significantly for non-stationary data and medium-to-long-term forecasts. The grey model works well for small/uncertain samples but suffers from declining accuracy over time due to weakening data correlation from accumulating disturbances. Kalman filters are robust and accurate (e.g., Hadamard-variance-based variants for rubidium clocks), yet remain vulnerable to environmental interference causing filter divergence.

This study proposes a novel hybrid model combining the metabolizing GM (1,1) model and a BP neural network to enhance satellite clock bias prediction accuracy. It operates in three stages: (1) initial short-term prediction by metabolizing GM (1,1), (2) BP network learning and forecasting of residuals, and (3) correction of GM (1,1) predictions using predicted residuals. Validation uses high-precision real clock bias data from Wuhan University's GNSS Analysis Center. Eight diverse GPS satellites are tested, and results consistently show superior accuracy, robustness, and effectiveness of the method.

2. Construction of Combined Prediction Model Based on Metabolizing GM (1,1) and BP Neural Network

2.1 GM (1,1) Model

The Grey Model employs accumulated generating operations and background-value whitening to transform intrinsically time-series data exhibiting nonlinear dynamics into approximately linear sequences, facilitating reliable forecasting even under conditions of scarce historical data. The underlying

algorithmic framework [6,9] is outlined below.:

Let there be a set of satellite clock bias time series:

$$x^{(0)} = \{x^{(0)}(1), x^{(0)}(2), \dots, x^{(0)}(n)\} \tag{1}$$

Generate the cumulative sequence corresponding to this temporal sequence:

$$x^{(1)} = \{x^{(1)}(1), x^{(1)}(2), \dots, x^{(1)}(n)\} \tag{2}$$

where $x^{(1)}(k) = \sum_{i=1}^k x^{(0)}(i)$.

Establish a first-order differential equation for this accumulated sequence:

$$\frac{dx^{(1)}}{dt} + ax^{(1)} = b \tag{3}$$

where parameter a is the development coefficient and parameter b is the grey action quantity.

For computational tractability, the differential equation is discretized into an equivalent difference equation.

$$x^{(0)}(k) + az^{(1)}(k) = b \tag{4}$$

where $z^{(1)}(k)$ is the sequence of neighboring average values derived from $x^{(1)}$, and $z^{(1)}(k) = \frac{1}{2}[x^{(1)}(k) + x^{(1)}(k-1)]$.

Using the least squares method, the estimated values \hat{a} and \hat{b} of parameters a and b can be obtained.

Define the matrix as:

$$\begin{bmatrix} 1 & z^{(1)}(2) \\ 1 & z^{(1)}(3) \\ \vdots & \vdots \\ 1 & z^{(1)}(n) \end{bmatrix} \begin{bmatrix} a \\ b \end{bmatrix} = \begin{bmatrix} x^{(0)}(2) \\ x^{(0)}(3) \\ \vdots \\ x^{(0)}(n) \end{bmatrix}, \text{ abbreviated as } BP = Y \tag{5}$$

The variables \hat{a} and \hat{b} are calculated using the ordinary least squares $P = (B^T B)^{-1} B^T Y$ estimation technique, yielding their corresponding fitted values.

With the estimated parameters \hat{a} and \hat{b} in hand, the forecasted values of the accumulated generating sequence can be derived analytically.

$$\hat{x}^{(1)}(k+1) = \left[x^{(0)}(1) - \frac{\hat{b}}{\hat{a}} \right] e^{-\hat{a}k} + \frac{\hat{b}}{\hat{a}}, \quad k = 0, 1, 2, \dots \tag{6}$$

As the sequence $x^{(1)}$ represents the cumulative sum of the original sequence $x^{(0)}$, the forecasting model for the satellite clock bias series is consequently established.

$$\begin{cases} \hat{x}^{(0)}(1) = \hat{x}^{(1)}(1) \\ \hat{x}^{(0)}(k+1) = \hat{x}^{(1)}(k+1) - \hat{x}^{(1)}(k) = (1 - e^{-\hat{a}}) \left[x^{(0)}(1) - \frac{\hat{b}}{\hat{a}} \right] e^{-\hat{a}k} \end{cases} \quad (7)$$

Based on this formula, the satellite clock bias at any future time can be predicted.

2.2 Metabolizing GM (1,1) Model

Insert new data $x^{(0)}(n+1)$ (obtained from GM (1,1) model prediction) while removing old data to obtain a new clock bias sequence.

$$x^{(0)} = \{x^{(0)}(2), x^{(0)}(3), \dots, x^{(0)}(n+1)\} \quad (8)$$

Treat this updated sequence as the new raw input and iteratively apply the preceding modeling procedures until the entire forecasting horizon is covered. [10]. This method has the advantages of requiring less data, short operation cycle and high prediction accuracy, and can achieve good results in satellite clock bias prediction [11].

The specific flowchart can be found in Figure 1:

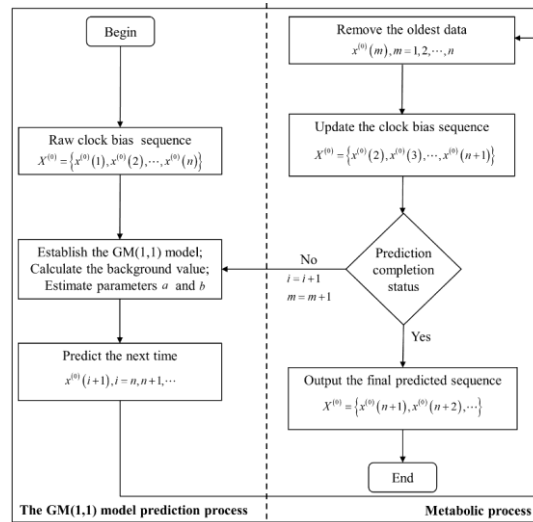


Figure 1: Prediction Procedure for Satellite Clock Bias Using the Metabolizing GM (1,1) Model

2.3 BP Neural Network

The BP neural network trains via alternating forward and backward propagation to iteratively adjust weights. It maps inputs to outputs using weighted nonlinear activation functions, enabling flexible, data-driven nonlinear transformation. Optimization progressively reduces the error between predicted and target outputs, achieving supervised learning. It comprises an input layer, one or more hidden layers, and an output layer, with inter-layer neuron connections but no intra-layer connections [12,13]. The neuron is its fundamental computational unit.

Each neuron computes a linear transformation of the prior layer's inputs—comprising weighted aggregation and bias addition—then passes the result through a nonlinear activation to generate the neuron's output—enabling learning of complex input–output mappings. Every synaptic connection has an associated learnable weight. Training relies on error backpropagation to iteratively update weights and biases until convergence. The core objective is to minimize prediction error through gradient-based optimization. Detailed principles and implementation steps are provided in references [12] and [14].

2.4 Combined Prediction Model

This study introduces a novel GPS satellite clock offset forecasting model that synergistically integrates a metabolizing GM (1,1) method with a backpropagation neural network. This method uses a small amount of clock bias data to establish a metabolizing GM (1,1) model and predicts for a certain period to obtain prediction values. The prediction residuals are obtained by subtracting the prediction values from the true values. Then, the prediction residuals are input into the established BP neural network for training to capture the variation patterns of the residuals and predict future residuals. Finally, the established metabolizing GM (1,1) is used for subsequent clock bias prediction, and the corresponding predicted residuals are added to obtain the combined model's clock bias prediction values. The forecast flowchart of the combined model is shown in Figure 2:

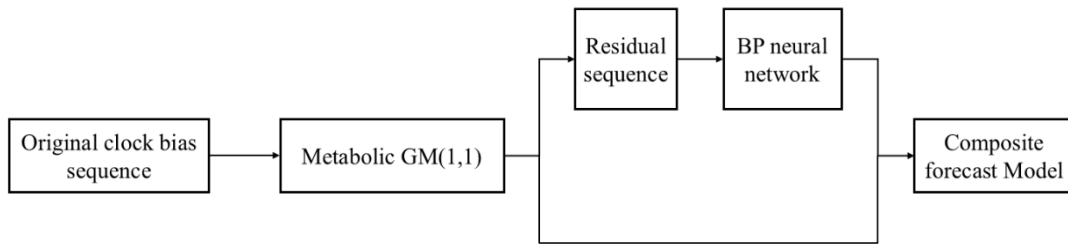


Figure 2: Flowchart of Combined Model Clock Bias Prediction

3. Experimental Evaluation and Discussion

3.1 Data Collection Origin

For model validation, this work utilizes high-accuracy GPS satellite clock bias measurements—sampled every 30 seconds—obtained from the Wuhan University GNSS Analysis Center’s product corresponding to Day 1 of GPS Week 2377. The dataset employed in the experiments covers more than 30 satellites in orbit. Eight representative rubidium clock data from the GPS system were randomly selected for experiments: PRN03, PRN05, PRN10, PRN11, PRN15, PRN16, PRN22 and PRN27 (see Table 1 for details).

Table 1: Chosen Satellite-Specific Parameters

Satellite Designation	Type of Clock	Date of Launch	Clock Bias Trend	Linearity
PRN 03	II-F-Rb	October 29, 2014	Positive decreasing	Good
PRN 05	II-R-Rb	August 17, 2009	Negative decreasing	Poor
PRN 10	II-F-Rb	October 31, 2015	Negative decreasing	Good
PRN 11	III-A-Rb	June 17, 2021	Negative increasing	Good
PRN 15	II-R-Rb	October 17, 2007	Positive increasing	Fair
PRN 16	II-R-Rb	January 29, 2003	Positive increasing	Good
PRN 22	II-R-Rb	July 16, 2000	Negative increasing	Poor
PRN 27	II-F-Rb	May 15, 2013	Negative decreasing	Good

Figure 3 illustrates the temporal evolution of clock biases for eight selected satellites during a 4-hour continuous observation interval. The observation data shows that PRN03, PRN05, PRN10 and PRN27 show a decreasing trend, while PRN11, PRN15, PRN16 and PRN22 show an increasing trend. Notably, the clock bias curves of PRN05 and PRN22 exhibit significant nonlinear characteristics.

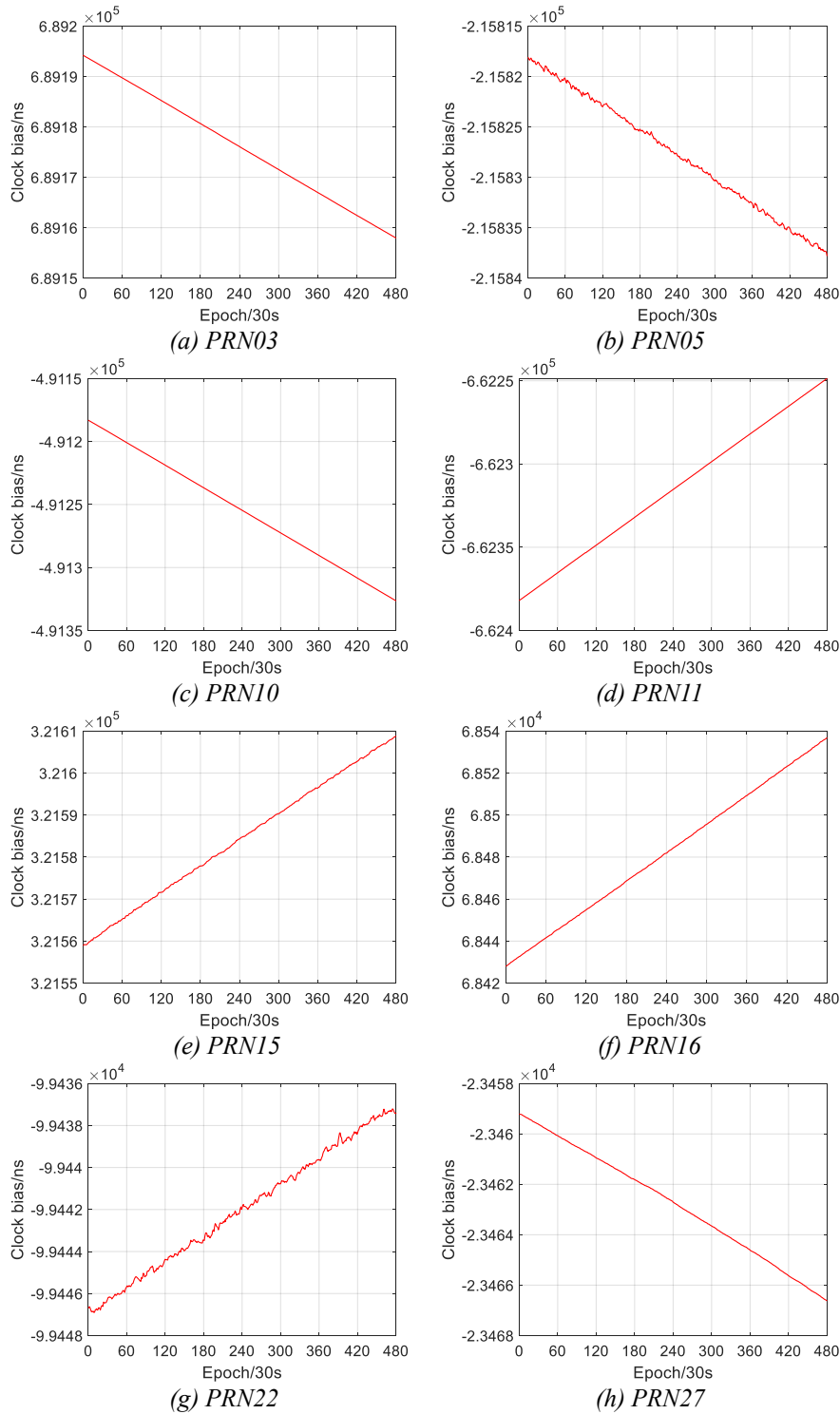


Figure 3: Chart of clock bias variation of the PRN03, PRN05, PRN10, PRN11, PRN15, PRN16, PRN22 and PRN27 satellites

3.2 Forecast Outcomes and Interpretation

This study built three clock bias prediction models—LPM, GM (1,1), and a hybrid model combining metabolic GM (1,1) with BP neural network—using 6-hour observation data. Two forecasting setups were tested: (i) 2-h ahead over 6-h horizon, and (ii) 2-h ahead over 18-h horizon. Prediction residuals were computed by subtracting Wuhan University’s GNSS Analysis Center high-precision reference clock bias values from model outputs. Accuracy and stability were evaluated using RMS error and error range (max–min residual). The equations used to compute the root-mean-square (RMS) error and the data range

are presented below:

$$RMS = \sqrt{\frac{1}{n} \sum_{i=1}^n (x_i - \hat{x}_i)^2} \tag{9}$$

$$Range = \max(x_i - \hat{x}_i) - \min(x_i - \hat{x}_i) \tag{10}$$

Figures 4–5 present the temporal profiles of prediction errors for all models under each forecasting scenario, while Tables 2–4 summarize the corresponding error statistics.

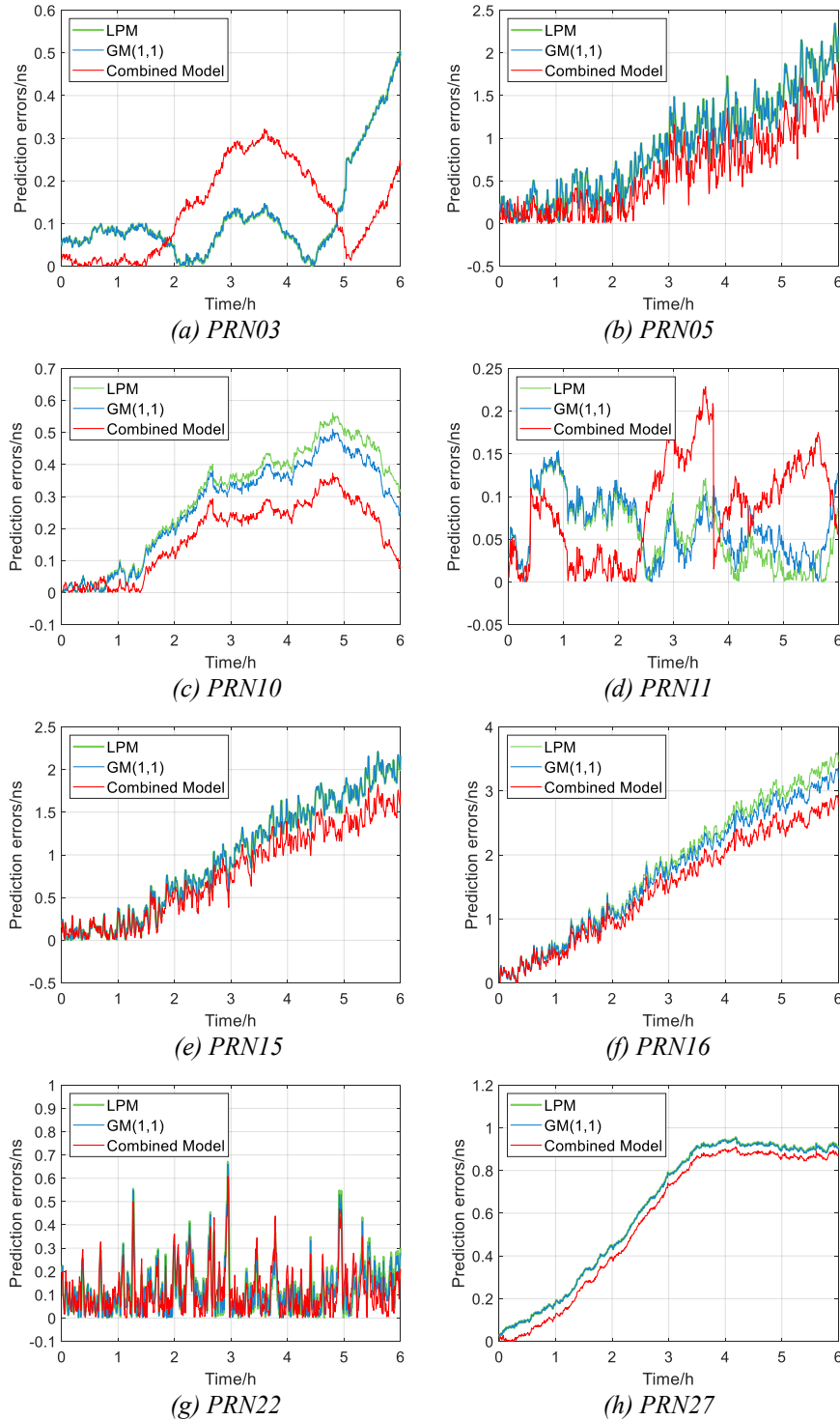


Figure 4: 2 h forecast of 6 h satellite clock bias variation

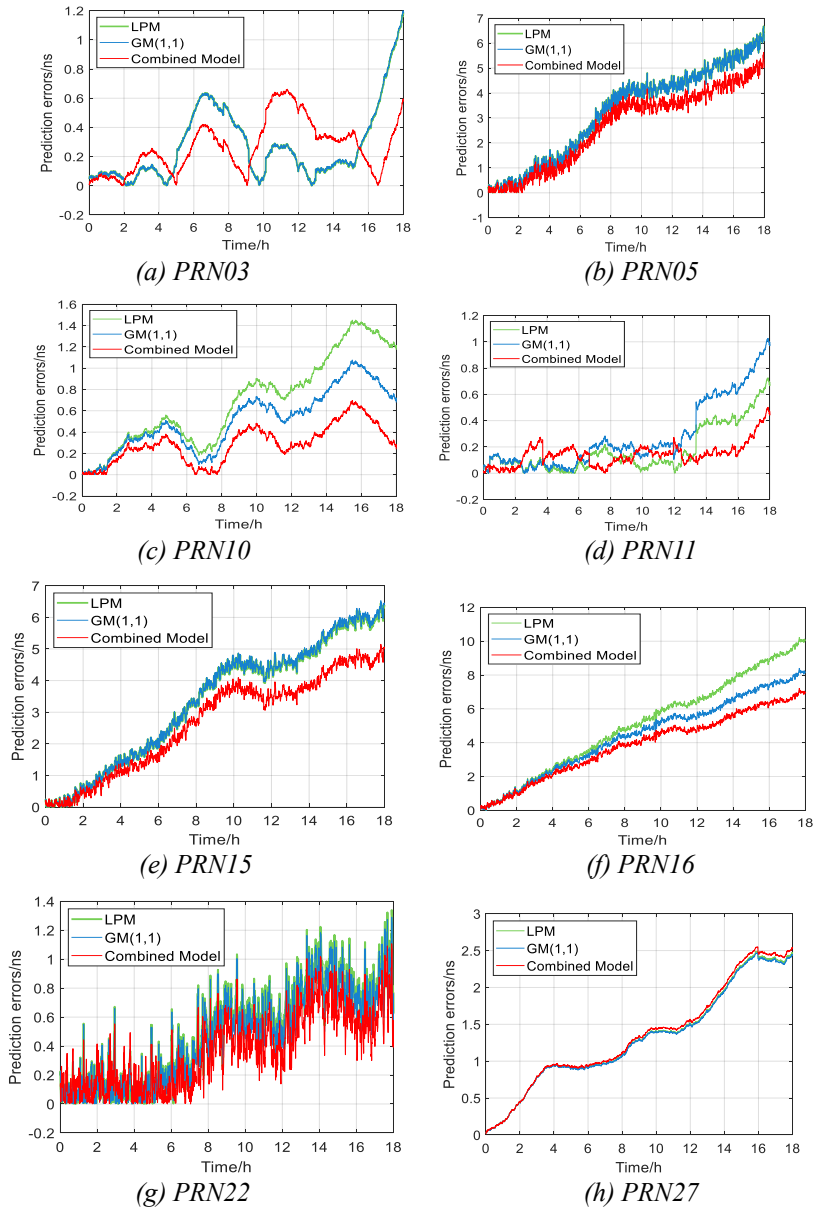


Figure 5: 2 h forecast of 18 h satellite clock bias variation

Table 2: Statistical Evaluation of 6 h Satellite Clock Bias Forecasts Using a 2 h Prediction Interval (unit: ns)

Model	Evaluation indicators	PRN 03	PRN 05	PRN 10	PRN 11	PRN 15	PRN 16	PRN 22	PRN 27	Mean
LPM	RMS	0.16	1.07	0.34	0.07	1.18	2.09	0.16	0.70	0.72
	Range	0.50	2.35	0.56	0.15	2.21	3.59	0.67	0.93	1.37
GM (1,1)	RMS	0.16	1.07	0.31	0.07	1.18	1.97	0.16	0.70	0.70
	Range	0.50	2.34	0.51	0.15	2.21	3.34	0.66	0.93	1.33
Combined Model	RMS	0.15	0.75	0.21	0.11	1.00	1.76	0.15	0.68	0.60
	Range	0.29	1.86	0.38	0.24	1.88	2.94	0.61	0.94	1.14

Table 3: Statistical Evaluation of 18 h Satellite Clock Bias Forecasts Using a 2 h Prediction Interval (unit: ns)

Model	Evaluation indicators	PRN 03	PRN 05	PRN 10	PRN 11	PRN 15	PRN 16	PRN 22	PRN 27	Mean
LPM	RMS	0.37	3.74	0.81	0.25	3.85	5.84	0.60	1.49	2.12
	Range	1.19	6.69	1.45	0.73	6.45	10.22	1.34	2.47	3.82
GM (1,1)	RMS	0.37	3.74	0.59	0.39	3.88	5.01	0.57	1.48	2.00
	Range	1.20	6.67	1.08	1.03	6.53	8.39	1.30	2.46	3.58
Combined Model	RMS	0.33	3.11	0.33	0.17	3.11	4.34	0.44	1.53	1.67
	Range	0.69	5.62	0.69	0.49	5.17	7.22	1.10	2.55	2.94

Table 4 The average forecast accuracy and improvement rate of the three forecasting methods for each model

Model	RMS	Range
Combined Model	1.14	2.04
LPM	1.42	2.60
Improvement (%)	19.72	21.54
GM (1,1)	1.35	2.46
Improvement (%)	15.56	17.07

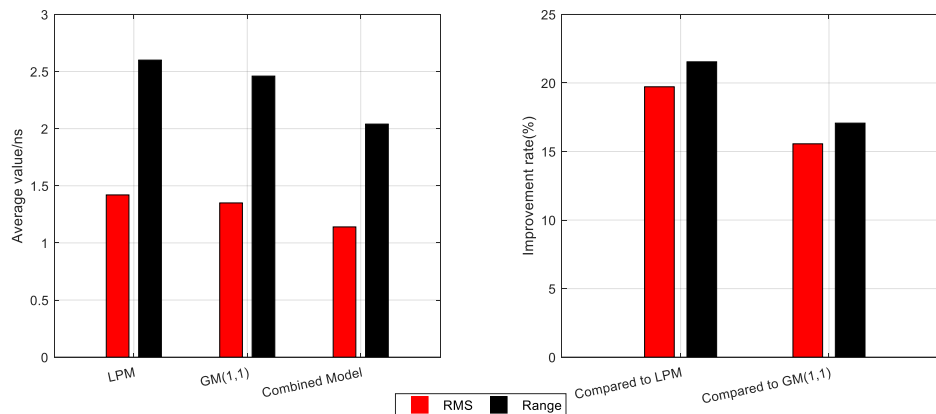


Figure 6: Average prediction accuracy, stability, and enhancement ratio across the three forecasting schemes

Based on Figures 4-6 and Tables 2-4, The results clearly indicate that, across all three forecasting setups, the combined model achieves the best overall performance in both accuracy and stability. In the 2h data predicting 6h method, the mean forecasting error of the linear polynomial model is 0.72 ns, and mean prediction consistency is 1.37 ns; the mean forecasting error of the grey model is 0.70 ns, and mean prediction consistency is 1.33 ns; the mean forecasting error of the combined model is 0.60 ns, and mean prediction consistency is 1.14 ns. In the 2h data predicting 18h method, the mean forecasting error of the linear polynomial model is 2.12 ns, and mean prediction consistency is 3.82 ns; the mean forecasting error of the grey model is 2.00 ns, and mean prediction consistency is 3.58 ns; the mean forecasting error of the combined model is 1.67 ns, and mean prediction consistency is 2.94 ns. The mean forecasting error and mean prediction consistency of the two prediction methods are 1.42 ns and 2.60 ns for the linear polynomial model, 1.35 ns and 2.46 ns for the grey model, and 1.14 ns and 2.04 ns for the combined model. Compared to the linear polynomial model and the grey model, the combined model demonstrates enhancement rates of 19.72% and 15.56% in mean prediction accuracy, and 21.54% and 17.07% in stability, respectively.

As illustrated in Figures 4-5 and summarized in Tables 2-3, for a fixed dataset size, prediction accuracy and stability generally degrade as the forecasting horizon increases—i.e., shorter prediction intervals yield higher mean accuracy and greater consistency. In short-term forecasting scenarios, while the hybrid model achieves the best overall performance in terms of average accuracy and stability, the error trajectories of all three models remain comparatively similar, thereby limiting the observable advantage of the integrated approach. Moreover, the hybrid method entails substantial computational overhead—particularly during residual modeling, training, and fitting—which leads to prolonged runtime and inefficient resource utilization. Consequently, its application is not advised for short-horizon predictions where computational efficiency and timeliness are critical.

4. Conclusion

This study proposes a novel hybrid forecasting approach that combines an enhanced GM (1,1) model with a back-propagation (BP) neural network to improve both accuracy and stability in predicting GPS satellite clock biases. The approach operates in three sequential stages: First, the metabolizing GM (1,1) model generates initial short-term forecasts of clock bias. Second, the residuals—i.e., discrepancies between these forecasts and actual observed values—are computed and fed as training data into the BP network to learn and model residual dynamics. Third, the GM (1,1) model is applied again to forecast future clock bias values, which are then refined by adding the BP-predicted residuals, yielding final

hybrid estimates. By leveraging the strengths of both models—GM (1,1)'s strong performance with limited historical data and the BP network's capacity for nonlinear residual correction—the proposed method achieves superior accuracy and consistency compared to standalone models. Empirical evaluation confirms its particular efficacy in long-horizon forecasting under data-scarce conditions. Nevertheless, due to the inherent non-determinism and approximation nature of BP-based residual modeling—where learned patterns may not fully capture all residual behaviors and repeated runs yield slightly varying outcomes—the resulting mean prediction accuracy and stability exhibit modest fluctuations across trials. Despite this variability, the hybrid model consistently outperforms both the conventional linear polynomial and classical grey models across all evaluation metrics.

Acknowledgements

This study is supported by the National Natural Science Foundation of China (No. 12403080), the China Postdoctoral Research Performance Evaluation and Assessment Funding Project (YJC20251197), the China Postdoctoral Science Foundation Funded Project (No.2024M764304), the Postdoctoral Fellowship Program of CPSF (No. GZC20233565) and the Natural Science Basic Research Program in Shaanxi Province of China (No.2023-JC-QN-0027).

References

- [1] Lu C L, Lei Y, Zhao D N. *Design and Implementation of GNSS Satellite Clock Performance Analysis and Prediction Software*[J]. *GNSS World of China*, 2025, 50(05): 51-59.
- [2] Yu Y, Yang C P, Ding Y, et al. *A hybrid short-term prediction model for BDS-3 satellite clock bias supporting real-time applications in data-denied environments*[J]. *Remote Sensing*, 2025, 17(16):2888-2913.
- [3] Ma Z X, Yang L, Jia X L, et al. *Improved Satellite Clock Difference Prediction Method Based on Polynomial Model*[J]. *GNSS World of China*, 2016, 41(02): 27-31+37.
- [4] Yu Y, Huang M, Duan T, et al. *Satellite clock offset forecasting using a combination of particle swarm optimization and weighted grey regression* [J]. *Journal of Harbin Institute of Technology*, 2020, 52(10): 144-151.
- [5] Yu Y, Huang M, Wang C Y, et al. *A new BDS-2 satellite clock bias prediction algorithm with an improved exponential smoothing method* [J], *Applied Sciences*,2020,10(21):7456-7479.
- [6] Wang Y H, Song X L, Gong J J. *Application of Error-Corrected Grey Model in Navigation Satellite Clock Difference Prediction*[J]. *Journal of Time and Frequency*, 2025, 48(01): 68-78.
- [7] Zhang J R, Tang L N. *Rubidium Atomic Clock Difference Prediction Based on Improved Kalman Filter*[J]. *Journal of Xi'an University of Posts and Telecommunications*, 2019, 24(05): 1-5.
- [8] Yu Y, Zhang H J, Li X H, et al. *Medium and Short-term Prediction of GPS Satellite Clock Difference Based on GM (1,1) and MECM Combined Model*[J]. *Acta Astronomica Sinica*, 2018, 59(03): 19-30.
- [9] Li T, Wang J M, Zhang W C. *Establishment of BDS Clock Difference Combined Prediction Model Based on Entropy Weight Method*[J]. *Journal of Navigation and Positioning*, 2022, 10(04): 65-72.
- [10] Guo R X, Yi M, Gao Y P. *Research on Real-time GPS Satellite Clock Difference Prediction Based on Metabolizing Grey Model*[J]. *Beijing Surveying and Mapping*, 2016, (06): 22-26.
- [11] Sun G Q. *Prediction of Slope Foundation Bearing Capacity Based on Metabolizing Grey GM (1,1) Model*[J]. *Guangdong Building Materials*, 2025, 41(11): 103-106.
- [12] Li Y F, Shi S H. *Satellite Clock Difference Prediction Based on GM (1,1) and BP Neural Network*[J]. *Electronic Design Engineering*, 2020, 28(09): 7-11.
- [13] Liu W C, Zhou Z G. *Research on GPS Satellite Clock Difference Combined Prediction Model*[J]. *Geomatics & Spatial Information Technology*, 2023, 46(10): 118-120+124+127.
- [14] Fang C Z. *Research on Wind Power Combined Prediction Based on BP Neural Network and Support Vector Machine*[D]. *Inner Mongolia University of Science and Technology*, 2021.